iScience

CellPress
OPEN ACCESS

Article

Rutin alleviates ventilator-induced lung injury by inhibiting NLRP3 inflammasome activation

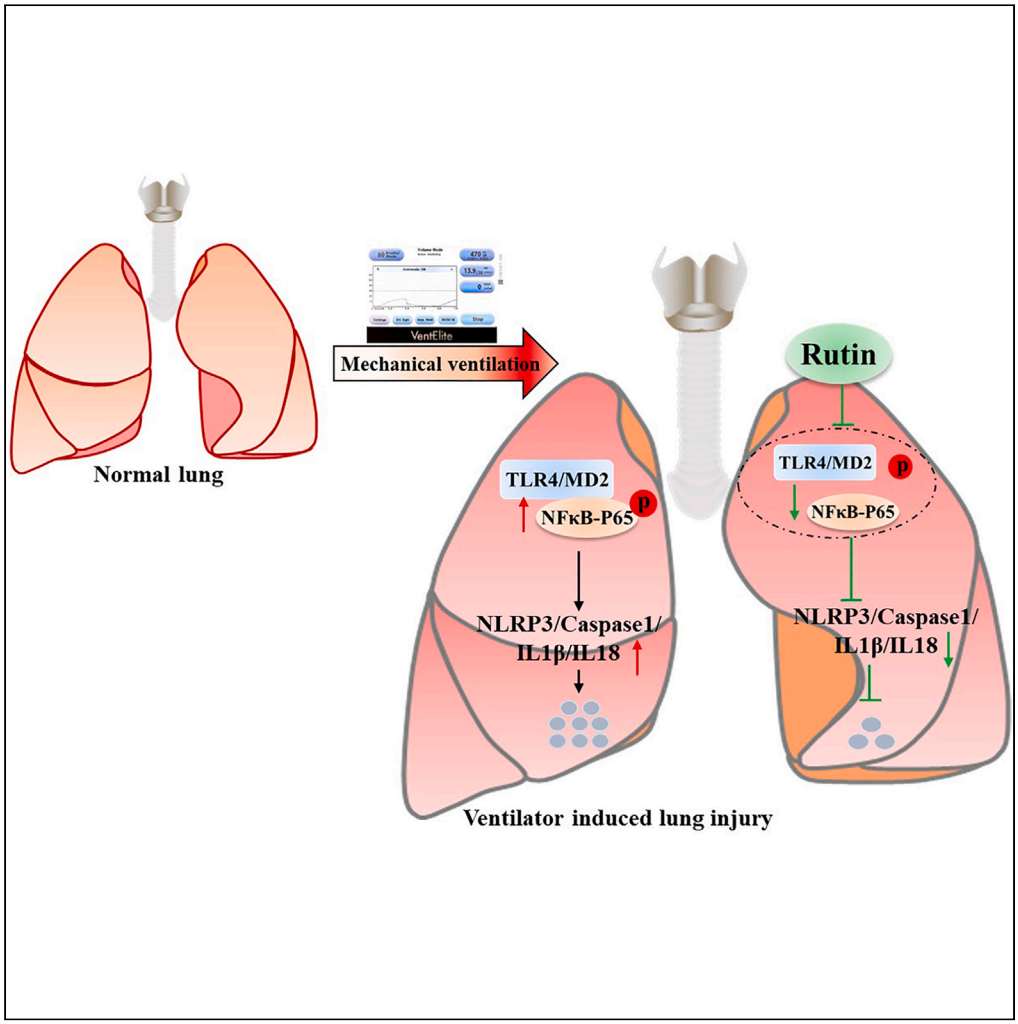

Shengsong Chen, Yu Bai, Jingen Xia, Yi Zhang, Qingyuan Zhan

czzhangyi1985@126.com (Y.Z.)
drzhanqy@163.com (Q.Z.)

Highlights

Rutin treatment improved VILI in mice

Rutin relieved NLRP3 activation by regulating macrophage polarization in VILI

Rutin inhibited the activation of the TLR4/NF-κB-P65 pathway in VILI

Chen et al., iScience *26*, 107866
October 20, 2023
https://doi.org/10.1016/j.isci.2023.107866

iScience

CellPress
OPEN ACCESS

Article

Rutin alleviates ventilator-induced lung injury by inhibiting NLRP3 inflammasome activation

Shengsong Chen,[1,2,3,4,5,6,7,8] Yu Bai,[1,2,3,4,5,6,8] Jingen Xia,[1,3,4,5,6] Yi Zhang,[1,3,4,5,6,*] and Qingyuan Zhan[1,2,3,4,5,6,9,*]

SUMMARY

Whether rutin relieves ventilator-induced lung injury (VILI) remains unclear. Here, we used network pharmacology, bioinformatics, and molecular docking to predict the therapeutic targets and potential mechanisms of rutin in the treatment of VILI. Subsequently, a mouse model of VILI was established to confirm the effects of rutin on VILI. HE staining showed that rutin alleviated VILI. TUNEL staining showed that rutin reduced apoptosis in the lung tissue of mice with VILI, and the same change was observed in the ratio of Bax/Bcl2. Furthermore, rutin reduced the expression of NLRP3, ASC, Caspase1, IL1β, and IL18 in the lung tissues of mice with VILI. Mechanistically, rutin suppressed the TLR4/NF-κB-P65 pathway, which promoted the M1 to M2 macrophage transition and alleviated inflammation in mice with VILI. Rutin relieved NLRP3 inflammasome activation by regulating M1/M2 macrophage polarization and inhibiting the activation of the TLR4/NF-κB-P65 pathway, resulting in the amelioration of VILI in mice.

INTRODUCTION

Mechanical ventilation (MV) is an essential therapeutic measure to support life in patients with respiratory failure.[1,2] Unfortunately, inappropriate and prolonged MV can contribute to lung injury known as ventilator-induced lung injury (VILI), multisystem organ failure and death.[3] The pathogenesis of VILI is complex and not fully clarified. In addition, there is a lack of effective strategies to prevent VILI. Accordingly, exploring the etiopathogenesis and preventive measures of VILI is urgently needed.

Ventilator-induced repeated alveolar hyperextension and collapse, which is known as volutrauma, barotrauma, and atelectrauma, may contribute to mechanical stimulation and biological signal transduction.[4–6] This so-called mechanical-biological conduction is the main mechanism of the occurrence and development of VILI. Evidence suggests that MV induces the release of a variety of mediators and activates signaling pathways, promoting reactive oxygen species production and the immune inflammatory response, ultimately leading to lung injury.[4,5] In recent years, researchers have gained further insight into the biotrauma of VILI, which is defined as the release of inflammatory mediators, monocyte/macrophage infiltration and recruitment, infiltration of leukocytes and neutrophils, and initiation of local inflammatory processes and cell apoptosis through upregulated the ratio of Bcl2-associated protein x (Bax)/B-cell lymphoma 2 (Bcl2) in the lung, resulting in lung injury.[1,4,5,7,8] Furthermore, systemic inflammatory responses are also triggered when inflammatory mediators and inflammatory signals spill over from the alveolar spaces into the systemic circulation during MV, causing distant organ dysfunction and even death.[4,5,9] Therefore, inhibition of the inflammatory response is an important strategy for the prevention of VILI.

Rutin, which is also known as rutoside and vitamin P, is a citrus flavonoid glycoside consisting of the flavonol quercetin and the disaccharide rutinose.[10–12] Rutin has many biological activities and pharmacological effects, including anti-inflammatory, antibacterial, antioxidant, antiapoptotic, detoxification, lipid-lowering, vasodilation, and antitumor effects.[11–13] Clinically, rutin is widely used to reduce blood pressure, prevent cerebral infarction, and treat nephritis and bronchitis.[12] Previous studies confirmed that rutin prevents a variety of inflammatory diseases, such as colitis, nephrotoxicity, and cardiac inflammation.[12,14–16] Interestingly, rutin has also been reported to alleviate acute lung injury.[17–19] For example, rutin improved endotoxin-induced acute lung injury by inhibiting iNOS and vascular cell adhesion molecular-1(VCAM-1) expression.[17] Rutin decreased lipopolysaccharide-induced acute lung injury by inhibiting the nuclear factor kappa-B (NF-κB) pathway and AKT pathway.[18,19] VILI is closely related to the inflammatory response. Therefore, we speculated that rutin treatment may alleviate VILI.

[1]Department of Pulmonary and Critical Care Medicine, Center of Respiratory Medicine, China-Japan Friendship Hospital, No 2, East Yinghua Road, Chaoyang District, Beijing 100029, P.R.China
[2]Peking Union Medical College, Chinese Academy of Medical Sciences, No 9 Dongdan Santiao, Dongcheng District, Beijing 100730, P.R.China
[3]National Center for Respiratory Medicine, No 2, East Yinghua Road, Chaoyang District, Beijing 100029, P.R.China
[4]Institute of Respiratory Medicine, Chinese Academy of Medical Sciences, No 2, East Yinghua Road, Chaoyang District, Beijing 100029, P.R.China
[5]National Clinical Research Center for Respiratory Diseases, No 2, East Yinghua Road, Chaoyang District, Beijing 100029, P.R.China
[6]WHO Collaborating Center for Tobacco Cessation and Respiratory Diseases Prevention, No 2, East Yinghua Road, Chaoyang District, Beijing 100029, P.R.China
[7]Senior author
[8]These authors contributed equally
[9]Lead contact
*Correspondence: czzhangyi1985@126.com (Y.Z.), drzhanqy@163.com (Q.Z.)
https://doi.org/10.1016/j.isci.2023.107866

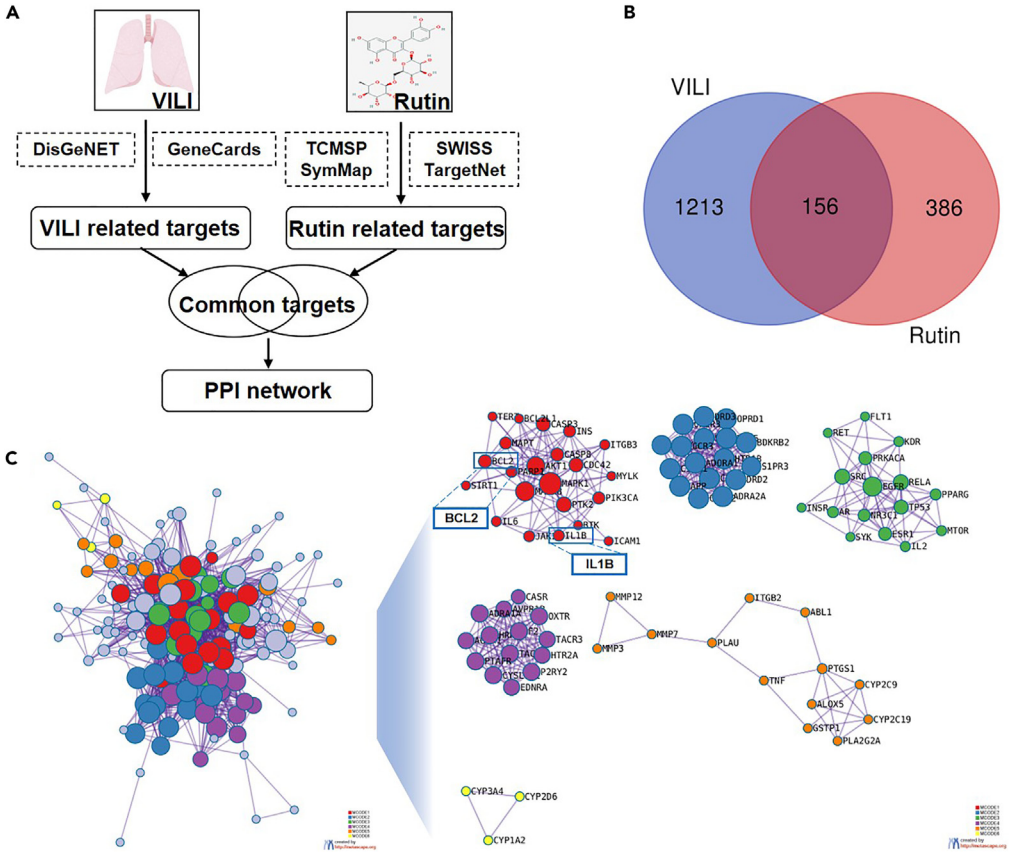

Figure 1. Potential target analysis of rutin in the treatment of VILI

(A) Network pharmacology analysis of rutin in the treatment of ventilator-induced lung injury (VILI).

(B) Venn analysis of common targets of rutin in the treatment of VILI.

(C) PPI analysis of connected network components.

In the present study, network pharmacology was used to identify potential common targets and mechanisms of rutin in the treatment of VILI. Then, we established a mouse model of VILI to explore the effect of rutin. Our findings may provide a novel basis for the development of treatments for VILI.

RESULTS

Potential target analysis of rutin in the treatment of VILI

The PubChem database was first used to search the 2D chemical structure of rutin (Figure 1A). Then, we explored potential targets of rutin in the treatment of VILI based on the aforementioned network pharmacological target fishing approach (Figure 1A). A total of 1369 VILI targets from two disease-related databases and a total of 542 rutin targets from four pharmacological databases were screened. A total of 156 common targets of rutin in the treatment of VILI were obtained by Venn analysis (Figure 1B). To further explore the mechanism of rutin in the treatment of VILI at the protein level, we constructed a PPI network model with the 156 common targets. Eighty-five protein spots were screened, and inflammation- and apoptosis-related proteins, such as Bcl2 and IL1β, accounted for a large proportion (Figure 1C).

Function and pathway enrichment analysis of the rutin-VILI target network

Gene Ontology (GO) analysis was performed to enrich the functions of the rutin-VILI target network, and the top 30 BP, molecular function (MF), and CC terms are displayed in bubble charts. There were 533 enrichment processes related to BP, which included signal transduction, inflammatory response, collagen catabolic process, negative regulation of apoptotic process, positive regulation of cell proliferation, leukocyte migration, positive regulation of protein phosphorylation, phospholipase C-activating G-protein coupled receptor signaling pathway, positive regulation of cell migration, and positive regulation of NF-κB transcription factor activity (Figure 2A). There were 115 enrichment processes related to the MF, which included drug binding, transmembrane receptor protein tyrosine kinase activity, kinase activity, nonmembrane spanning protein tyrosine kinase activity, 3′,5′-cyclic-AMP phosphodiesterase activity, protein kinase activity, iron ion binding, receptor

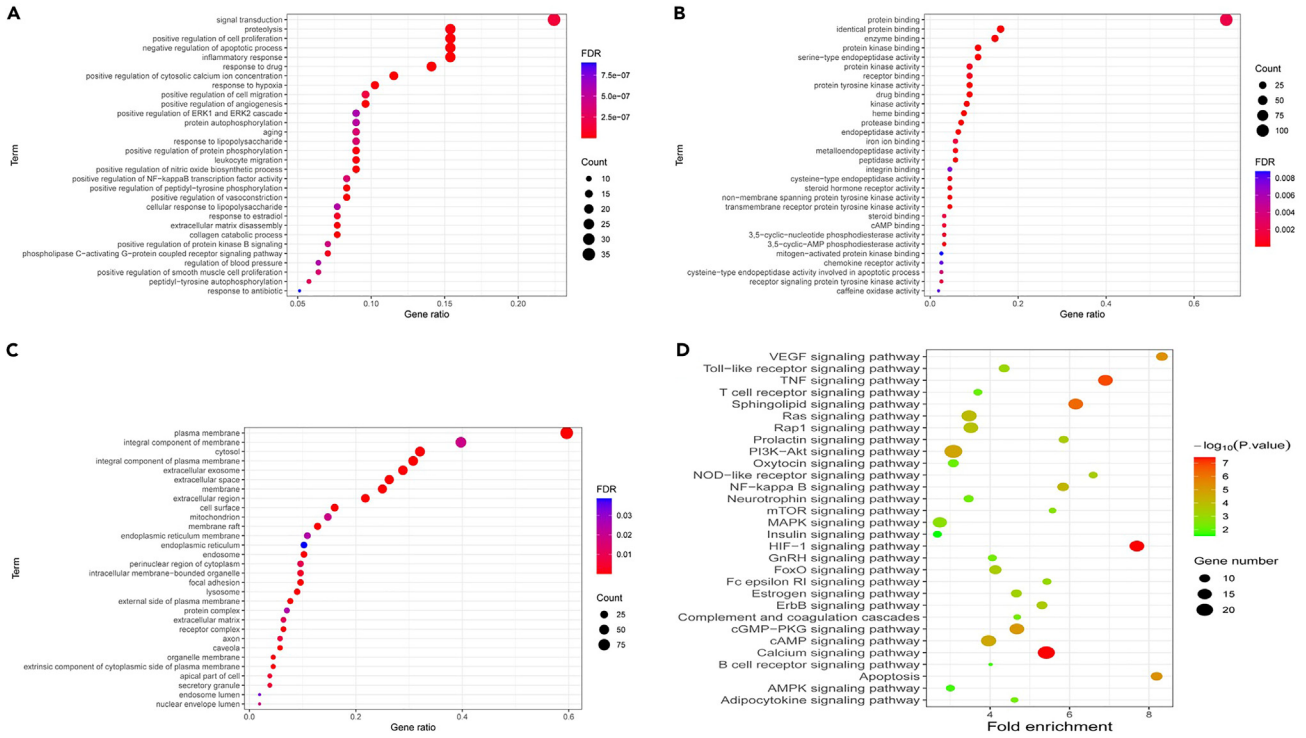

Figure 2. Functional and pathway enrichment analysis of the rutin-VILI target network

(A) GO biological process (BP) enrichment analysis.

(B) GO molecular function (MF) enrichment analysis.

(C) GO cellular component (CC) enrichment analysis.

(D) KEGG enrichment analysis.

signaling protein tyrosine kinase activity, protein binding, and chemokine receptor activity (Figure 2B). There were 61 enrichment processes related to CC, including plasma membrane, lysosome, receptor complex, cytosol, organelle membrane, intracellular membrane-bound organelle, extracellular matrix, nuclear envelope lumen, mitochondrion, and endoplasmic reticulum (Figure 2C). The size of the nodes indicated how many target genes were associated, and the colors from blue to red reflected the p values from high to low in the bubble graph, respectively. These results suggested that the inflammatory response and apoptosis played important roles in the rutin-VILI target network.

KEGG enrichment analysis was used to reveal the potential therapeutic mechanism of the rutin-VILI target network, and the top 30 pathways are displayed in bubble charts. There were 119 KEGG pathways, including the TNF signaling pathway, apoptosis, PI3K-Akt signaling pathway, NF-κB signaling pathway, NOD-like receptor signaling pathway, Toll-like receptor signaling pathway, mTOR signaling pathway, adipocytokine signaling pathway, T cell receptor signaling pathway, and B cell receptor signaling pathway (Figure 2D). The size of the nodes indicates how many target genes are associated, and the colors from green to red reflect the p values from high to low in the bubble graph, respectively. Previous studies have confirmed that biotrauma is the main cause of VILI.[1,4,5,7] The TLR4/NF-κB pathway and macrophage activation promote the inflammatory response and contribute to the pathogenesis of VILI.[5,20] Furthermore, Rutin decreased lung injury by inhibiting the NF-κB pathway[18.] Therefore, we hypothesized that rutin may improve VILI by regulating the TLR4/NF-κB pathway and the inflammatory response.

Molecular docking analysis

Molecular docking analyses were performed to screen the binding affinity of rutin. A threshold value of −5.0 kcal/mol for binding energy was used to determine the binding stability between the receptor and ligand.[21,22] A lower binding energy indicates a more stable binding conformation between the receptor and ligand.[21,22] Seven core targets, including TLR4/MD2, P65, Caspase1, NLRP3, ASC, IL1β, and IL18, were screened to determine the binding energy of key components of rutin (Figures 3A–3G). The binding energies of key components of rutin with seven core targets are shown in Table 1. These results indicated that the effect of rutin on VILI may be related to NLRP3 inflammasome activation and the TLR4/NF-κB pathway.

Rutin alleviated VILI in mice

We constructed a mouse model of VILI to confirm whether rutin could alleviate VILI in our study (Figure 4A). HE staining was used to evaluate the severity of lung injury. Compared to the control group, mice in the VILI group had more alveolar collapse and thicker alveolar walls and

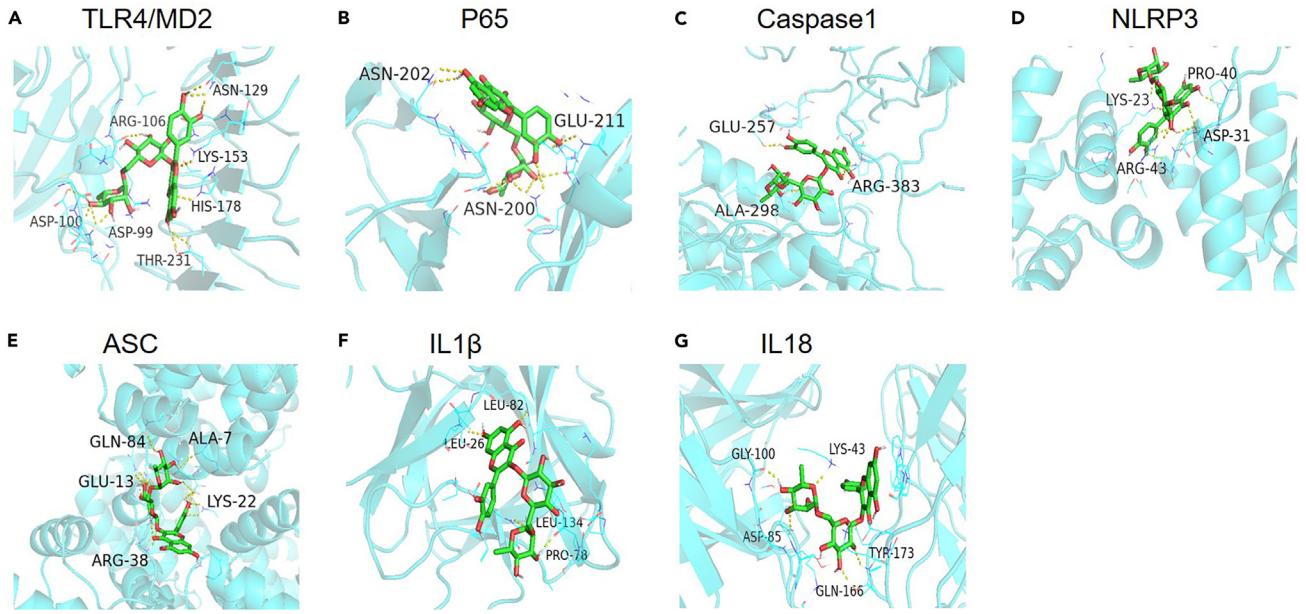

Figure 3. Molecular docking analysis

(A) Molecular docking result of TLR4/MD2.
(B) Molecular docking result of P65.
(C) Molecular docking result of Caspase1.
(D) Molecular docking result of NLRP3.
(E) Molecular docking result of ASC.
(F) Molecular docking result of IL1β.
(G) Molecular docking result of IL18.

septa; however, rutin pretreatment relieved VILI in mice compared to the VILI group ($p < 0.05$, Figures 4B and 4C). To further determine whether rutin improved VILI, TUNEL staining, immunohistochemistry (IHC), and western blotting were used to assess apoptosis in the lung tissues of mice with VILI. As expected, compared to the VILI group, mice in the VILI + rutin group had lower levels of apoptosis, as shown by TUNEL staining ($p < 0.05$, Figures 4D and 4E). Bcl2 is one of the anti-apoptotic Bcl-2 family members and Bax is one of pro-apoptotic Bax-like subfamily members, the ratio of Bax/Bcl2 is acted as the severity of cell apoptosis.[23] Consistently, rutin pretreatment reduced the ratio of Bax/Bcl2 in the lung tissues of mice with VILI, which was higher in the VILI group ($p < 0.05$, Figures 4F–4I). In addition, BALF was collected, protein concentration and WBC in BALF were measured. The results showed that mice in the VILI group had higher protein concentration and cell count than that in the control group and VILI+Rutin group ($p < 0.05$, Figures 4J and 4K).

Rutin alleviated NLRP3 inflammasome activation in the lung tissue of mice with VILI

Our previous studies showed that inflammation plays an important role in the occurrence and development of VILI.[24–27] The network pharmacology results showed that NLRP3 inflammasome activation played an important role in the rutin-VILI target network. We further detected whether rutin reduced NLRP3 inflammasome activation in the lung tissues of mice with VILI. IHC staining, western blotting and RT-PCR were used to detect the expression of inflammatory mediators (Figure 5A). The results showed that the expression of NLRP3 and ASC and Cleaved-caspase1 in the VILI group were higher than those in the control group and VILI+ rutin group ($p < 0.05$, Figures 5B–5F). A similar trend was also observed in the expression of IL1β and IL18, as shown by RT-PCR and ELISA ($p < 0.05$, Figures 5G and 5H).

Rutin regulated macrophage polarization in the lung tissue of mice with VILI

Previous studies have shown that rutin modulates macrophage polarization in lung tissues, inhibiting inflammatory responses.[28–30] Our previous study showed that macrophage polarization promoted ventilator-induced lung fibrosis.[27] Therefore, we hypothesized that rutin regulated macrophage polarization in the lung tissue of mice with VILI. If was used to evaluate the expression of iNOS and CD206 protein in mice with VILI, which are markers of M1 and M2 macrophages, respectively (Figure 6A). The results showed that compared to the control group, mice in the VILI group had higher levels of iNOS and lower levels of CD206; compared to the VILI group, the VILI + rutin group had lower levels of iNOS and higher levels of CD206 in lung tissues ($p < 0.05$, Figures 6B and 6C). This result suggested that rutin promoted the M1 to M2 macrophage switch in the lung tissues of mice with VILI.

Table 1. Binding energy of key components of rutin with core target

Ligand	Receptor	Gene	Affinity (kcal/mol)
5280505	2z64	TLR4/MD2	−8.915
5280505	1my5	P65	−7.705
5280505	6vie	CASPASE1	−8.384
5280505	3qf2	NLPR3	−7.199
5280505	2n1f	ASC	−8.095
5280505	8i1b	IL1B	−8.097
5280505	2VXT	IL18	−11.17

Rutin regulated TLR4/NF-κB pathways in the lung tissue of mice with VILI

An abundant amount of evidence suggested that the TLR4/NF-κB-P65 pathway was linked to macrophage polarization in inflammatory diseases.[31–33] KEGG enrichment analysis showed that the NF-κB pathway and Toll-like receptor pathway were associated with the rutin-VILI target network. Consequently, we investigated whether rutin regulated macrophage polarization in VILI by inhibiting the TLR4/NF-κB-P65 pathway. IHC staining, western blotting, and RT-PCR were used to detect the protein expression of TLR4, MD2, p-P65, and P65 (Figure 7A). The results showed that the expression of TLR4 and MD2 in the VILI group was significantly higher than that in the control group and VILI + rutin group ($p < 0.05$, Figures 7B–7F). The same trend was observed in the expression of p-P65 and P65 and the ratio of p-P65/P65 expression ($p < 0.05$, Figures 7B–7F). These results suggested that rutin may regulate macrophage polarization via the TLR4/NF-κB-P65 pathway in the lung tissue of mice with VILI.

DISCUSSION

VILI occurs due to inappropriate and prolonged MV, which can increase the incidence and mortality of critically ill patients.[3] Rutin is a glycoside of the bioflavonoid quercetin with various protective effects, including anti-inflammatory, antiapoptotic, antioxidant, antitumor, and cardiovascular protective effects.[11–13] In the present study, we observed that rutin alleviated NLRP3 inflammasome activation in the lung tissue of mice, promoted M1 to M2 macrophage switching and inhibited the TLR4/NF-κB-P65 pathway, resulting in the alleviation of VILI in mice.

MV causes macrophage polarization imbalance and the release of a variety of inflammatory mediators, initiating an inflammatory cascade response and leading to lung injury, distant organ dysfunction, and even death.[1,4,5,7] For example, MV activates the NLRP3 inflammasome, and then NLRP3 interacts with procaspase-1 through ASC to activate caspase-1, contributing to the production of the proinflammatory cytokines IL1β and IL18 and eventually causing VILI.[34,35] Rutin has been reported to have anti-inflammatory effects on many diseases, including lung injury.[10,17,18] However, whether rutin can fight VILI remains unclear. Therefore, in our study, we first predicted the common target genes of rutin in the treatment of VILI through network pharmacology and bioinformatics analysis. The results showed that 156 common target genes and 85 interaction protein spots were identified, including Bcl2 and IL1β. Subsequently, GO and KEGG analyses revealed that NOD-like receptor-related inflammation and apoptosis were related to the rutin-VILI target network. NLRP3, caspase1, ASC, IL1β, and IL18 were next screened by molecular docking analysis. According to the prediction results, we constructed a mouse model of VILI to confirm the effects of rutin. As we predicted, rutin alleviated NLRP3 inflammasome activation and apoptosis levels in the lung tissue of mice with VILI, resulting in the amelioration of lung injury. Our results were consistent with previous reports that inhibiting NLRP3 inflammasome activation attenuated lung damage.[34,35]

Emerging evidence suggests that M1/M2 macrophage polarization is the beginning of the inflammatory response.[4,20] MV induces biological signal transduction and activates alveolar macrophages.[4–6] Alveolar macrophages are the primary sources of inflammatory cytokines in response to MV and contribute to the pathogenesis of VILI. The NLRP3 inflammasome is then activated in alveolar macrophages, which then release IL1β and IL18, contributing to VILI.[36,37] Our previous study also showed that macrophage polarization promoted ventilator-induced lung fibrosis.[27] In this study, we observed that rutin alleviated NLRP3 inflammasome activation to alleviate lung injury. Next, we used IF staining to confirm that rutin promoted M1 to M2 macrophage polarization. Our data are consistent with previous results showing that rutin inhibited inflammatory responses and protected pulmonary tissue by promoting M1 to M2 macrophage polarization.[28–30] In short, our results demonstrated that rutin may mitigate inflammation by regulating macrophage polarization.

We further explored how rutin regulated macrophage polarization to reduce pulmonary NLRP3 inflammasome-related damage in mice with VILI. KEGG enrichment analysis was used to predict the therapeutic mechanism of the rutin-VILI target network, and the NF-κB signaling pathway, NOD-like receptor signaling pathway, and Toll-like receptor signaling pathway were identified. Moreover, molecular docking analysis showed that TLR4/MD2 and NF-κB-P65 may affect the binding energy of key components of rutin. The TLR4/NF-κB pathway has been reported to be activated when macrophages transform into the M1 type in mice with VILI.[5,20,38]

Rutin decreased lung injury by inhibiting the NF-κB pathway.[18] Therefore, we hypothesized that rutin could ameliorate VILI by regulating the TLR4/NF-κB pathway. We further investigated this hypothesis in a mouse VILI model. The trend was the same: rutin inhibited the TLR4/NF-κB-P65 pathway, reducing NLRP3 inflammasome-related lung injury. However, whether rutin attenuates VILI by directly inhibiting the TLR4/NF-κB-P65 pathway to inhibit alveolar macrophage polarization and decrease NLRP3 inflammasome activation is still needed to explore. More studies are needed to further confirm the underlying mechanism.

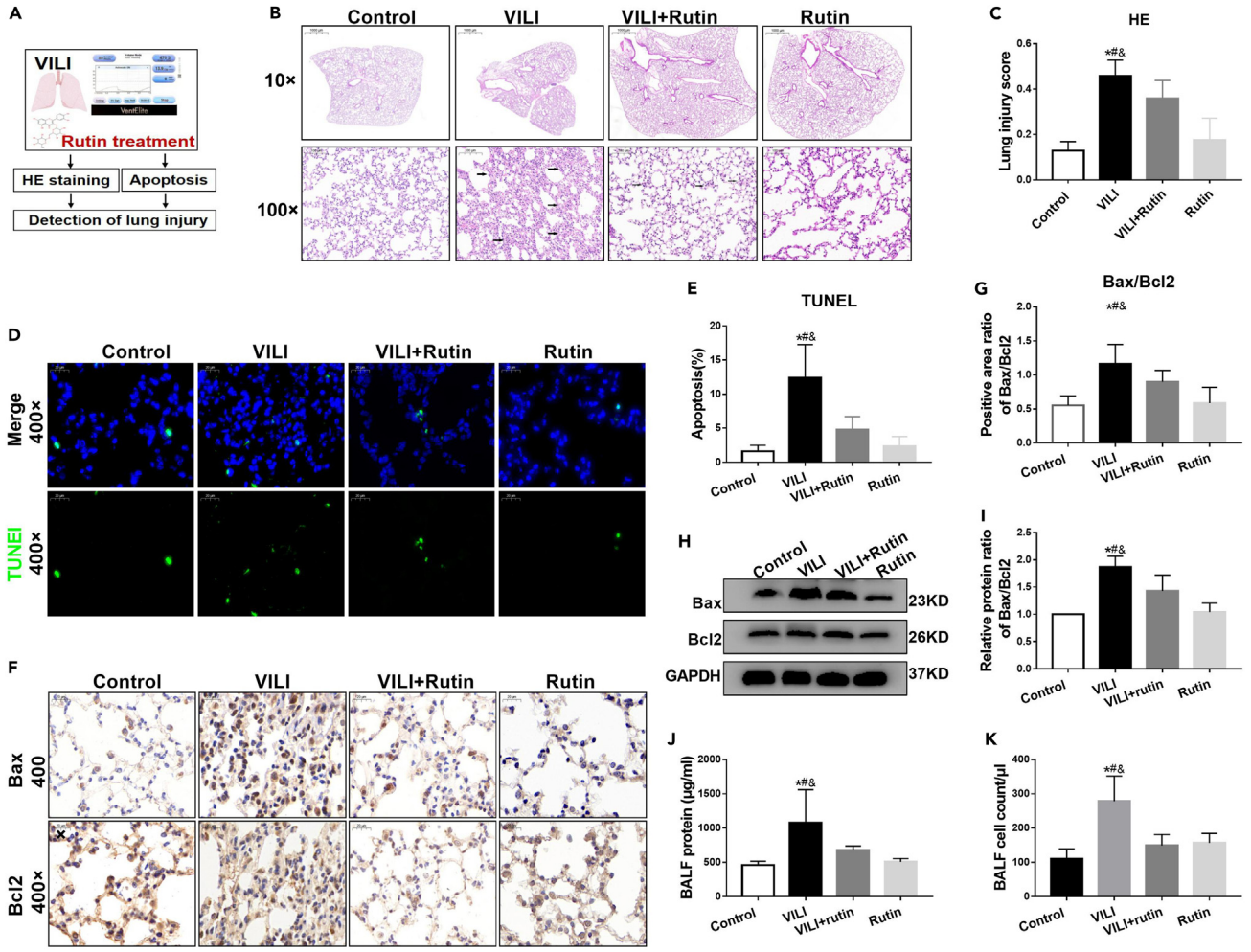

Figure 4. Rutin alleviated VILI in mice

(A) Flow chart showing rutin-mediated alleviation of VILI in mice.

(B) Hematoxylin and eosin (HE) staining of lung tissues in each group (original magnification × 1 and × 10). Arrows represent lung damage in HE staining.

(C) Quantification of the lung injury score in each group.

(D) TUNEL staining of apoptotic cells in each group (original magnification × 40).

(E) Quantification of apoptotic cells in each group.

(F) Immunohistochemical (IHC) staining of Bax and Bcl2 in each group (original magnification × 40).

(G) Quantification of the ratio of Bax/Bcl2 in each group.

(H) Western blot analysis of Bax and Bcl2 expression in each group.

(I) Quantification of the expression of Bax and Bcl2. (J) Protein concentration of BALF.

(K) WBC count of BALF. *$p < 0.05$ vs. Control group, $^{\#}p < 0.05$ vs. VILI+Rutin group, $^{\&}$ $p < 0.05$ vs. Rutin group.

Pulmonary fibrosis is another form of damage caused by MV that may increase mortality and poor quality of life in long-term survival.[39] Our previous studies observed that M2 macrophage polarization and TLR4/NF-κB-P65 pathway were related to MV-induced pulmonary fibrosis.[6,27]

Liu and his colleagues reported that NLRP3 inflammasome activation caused VILI and accelerated the progression of pulmonary fibrosis.[40] Verma found that a combination of podophyllotoxin and rutin alleviated radiation-induced pneumonitis and fibrosis through modulation of lung inflammation in mice.[41] Therefore, we speculate that rutin may improve MV-induced pulmonary fibrosis. Recently, researcher provided a review of the evidence of NLRP3 activation in pulmonary fibrosis and of NLRP3 inhibition in different animal models of fibrosis, and highlights the recent.[42]

Direct and indirect NLRP3 inhibitors, such as rutin, may be novel therapeutic approaches for MV-induced pulmonary fibrosis in future.

In conclusion, rutin reduced NLRP3 inflammasome activation by regulating M1/M2 macrophage polarization and inhibiting the activation of the TLR4/NF-κB-P65 pathway, resulting in the mitigation of VILI in mice. Our findings may provide new insight into rutin in the treatment of VILI by targeting its regulation.

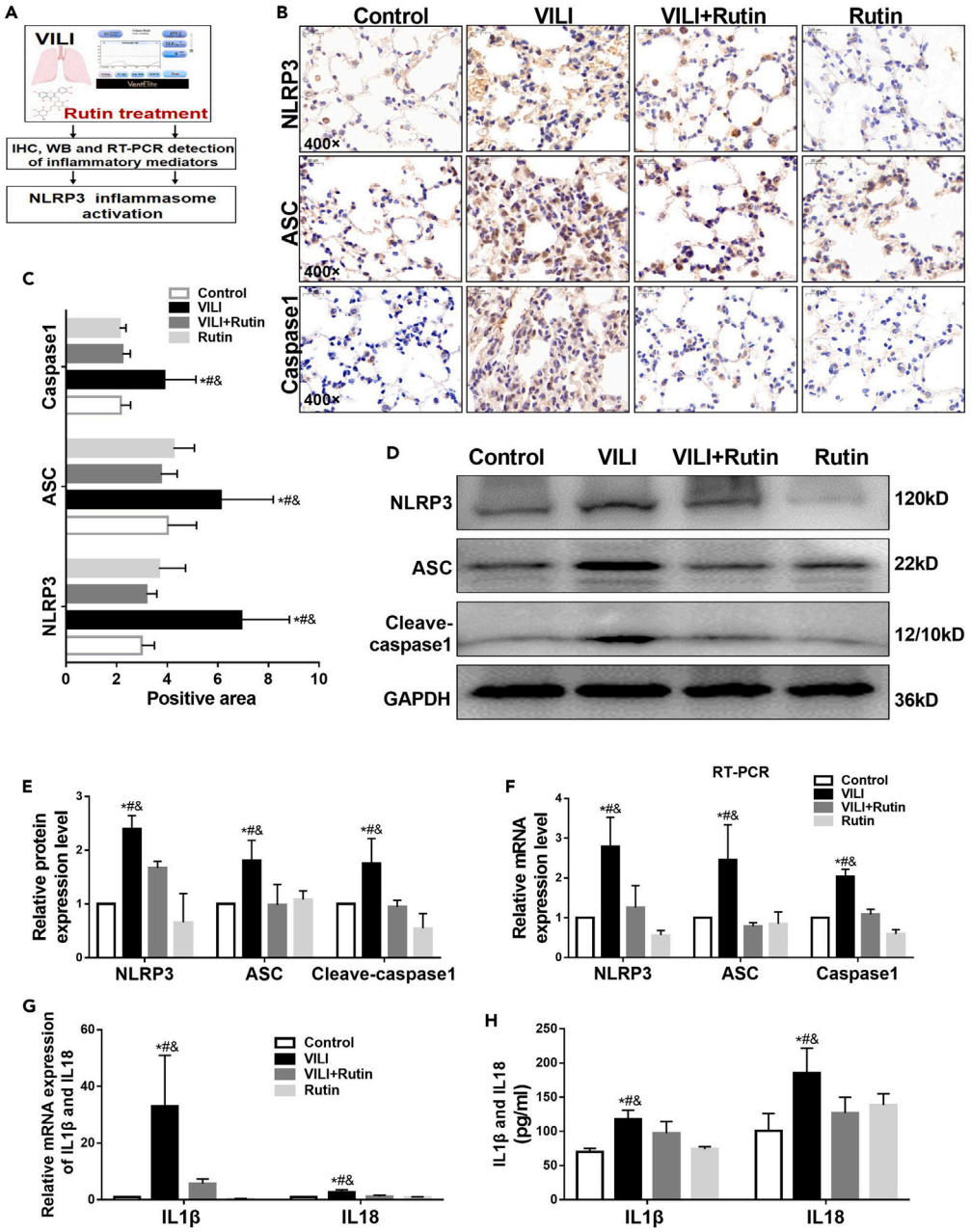

Figure 5. Rutin alleviated NLRP3 inflammasome activation in the lung tissue of mice with VILI

(A) Flow chart of rutin-mediated alleviation of NLRP3 inflammasome activation in mice with VILI.

(B) IHC staining of NLRP3, ASC, Caspase1, IL1β, and IL18 in each group (original magnification × 40).

(C) Quantification of positive staining for NLRP3, ASC, Caspase1, IL1β, and IL18 in each group.

(D) Western blot analysis of NLRP3, ASC and Cleave-caspase1 expression in each group.

(E) Quantification of the expression of NLRP3 and ASC and Cleave-caspase1.

(F and G) RT-PCR analysis of NLRP3, ASC, Caspase1, IL1β, and IL18.

(H) ELSIA analysis of IL1β and IL18. *$p < 0.05$ vs. Control group, $^{\#}p < 0.05$ vs. VILI+Rutin group, $^{\&}$ $p < 0.05$ vs. Rutin group.

Limitations of the study

Our study found that rutin improved VILI through inhibiting NLRP3 inflammasome activation *in vivo*. However, whether rutin could decrease mechanical stretch induced cellular injury *in vitro* is still unclear. In addition, whether rutin directly contributes to protective effect on pulmonary epithelial cell in VILI remains unclear. More studies are needed to uncover the action mechanism of rutin in VILI. The pathogenesis of

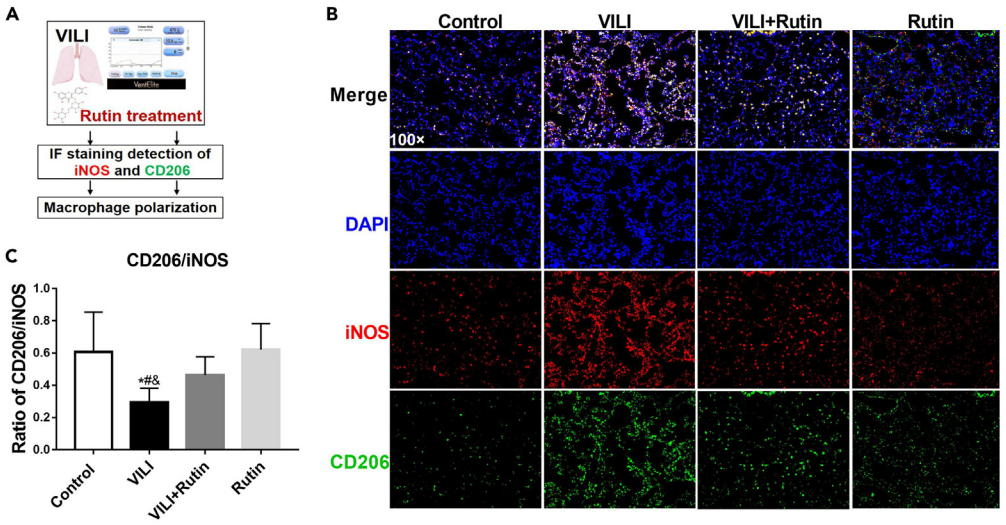

Figure 6. Rutin regulated macrophage polarization in the lung tissue of mice with VILI

(A) Flow chart of rutin-mediated regulation of macrophage polarization in mice with VILI.

(B) Immunofluorescence staining of iNOS and CD206 in each group (original magnification ×10 and × 40).

(C) Quantification of the ratio of CD206/iNOS in each group. *$p < 0.05$ vs. Control group, $^{\#}p < 0.05$ vs. VILI+Rutin group, $^{\&}p < 0.05$ vs. Rutin group.

mouse differs from that of humans. How long the patient may develop VILI after MV need further explore in future. VILI-related clinical studies should be conducted as soon as possible.

STAR★METHODS

Detailed methods are provided in the online version of this paper and include the following:

- KEY RESOURCES TABLE
- RESOURCE AVAILABILITY
  - Lead contact
  - Materials availability
  - Data and code availability
- EXPERIMENTAL MODEL AND SUBJECT DETAILS
  - Animals
  - Mouse model of VILI and rutin treatment
- METHOD DETAILS
  - Rutin chemical structures
  - Prediction of the targets of rutin
  - Prediction of targets for VILI
  - Prediction of therapeutic targets of rutin in the treatment of VILI
  - Construction of the protein–protein interaction (PPI) network
  - Gene Ontology and KEGG pathway analysis
  - Molecular docking
  - Hematoxylin-eosin (HE) staining
  - Measurement of protein concentrations and cell count in BALF
  - TUNEL staining
  - Immunofluorescence and immunohistochemical staining
  - Western blot analysis
  - Real-time PCR
- QUANTIFICATION AND STATISTICAL ANALYSIS

SUPPLEMENTAL INFORMATION

Supplemental information can be found online at https://doi.org/10.1016/j.isci.2023.107866.

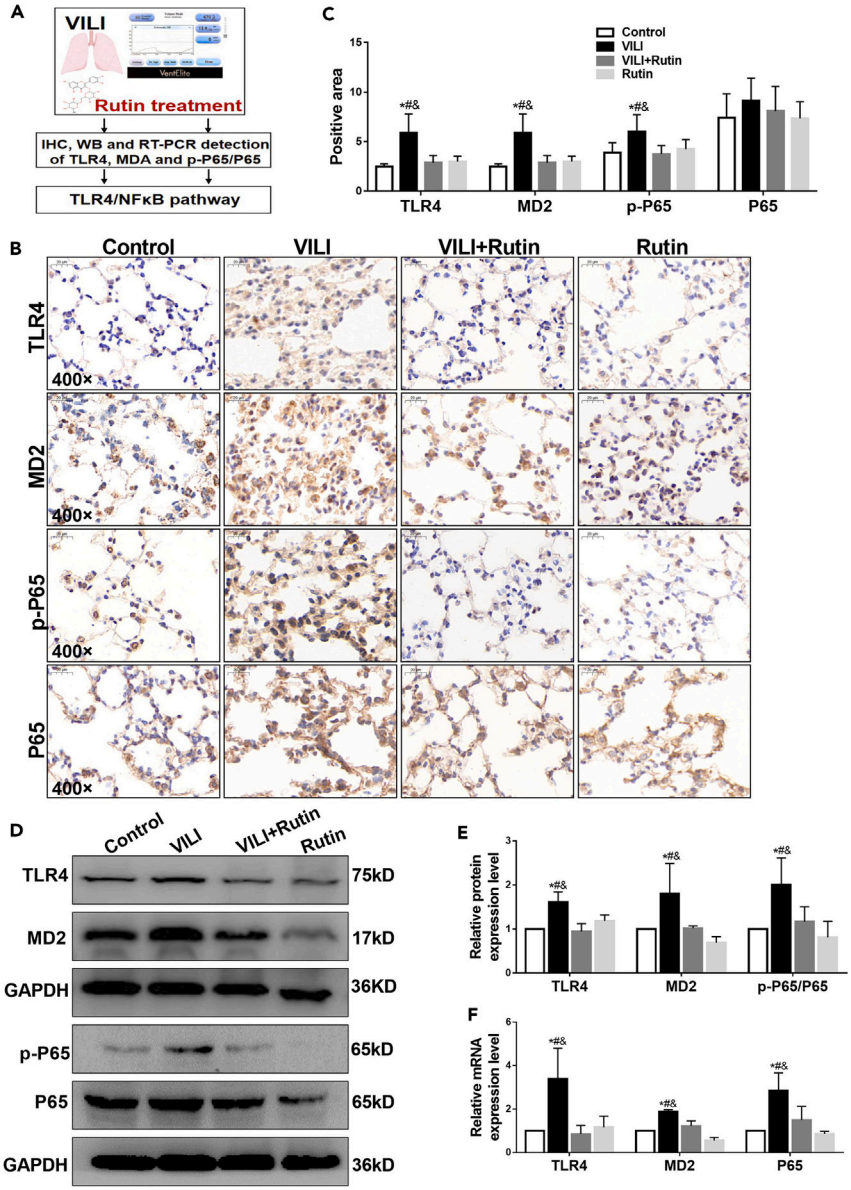

Figure 7. Rutin regulated the TLR4/NF-κB pathway in the lung tissue of mice with VILI

(A) Flow chart of rutin-mediated regulation of the TLR4/NF-κB pathway in mice with VILI.

(B) IHC staining of TLR4, MD2, p-P65, and P65 in each group (original magnification ×40).

(C) Quantification of positive staining for TLR4 and MD2 and the ratio of p-P65/P65 in each group.

(D) Western analysis of for TLR4, MD2, p-P65, and P65 protein expression in each group.

(E) Quantification of the expression of TLR4 and MD2 and the ratio of p-P65/P65.

(F) RT-PCR analysis of TLR4, MD2, and P65. *$p < 0.05$ vs. Control group, $^{\#}p < 0.05$ vs. VILI+Rutin group, $^{\&}p < 0.05$ vs. Rutin group.

ACKNOWLEDGMENTS

This work was supported by grants from the National Natural Science Foundation of China (Nos. 81870072).

AUTHOR CONTRIBUTIONS

Conceptualization, C.S.S.; Methodology, C.S.S., B.Y., and X.J.G.; Formal Analysis, C.S.S. and B.Y.; Investigation, C.S.S., B.Y. and X.J.G.; Writing – Original Draft, C.S.S.; Writing – Review & Editing, Z.Y. and Z.Q.Y.; Funding Acquisition, C.S.S., Z.Y., and Z.Q.Y.; Resources, C.S.S., B.Y., and X.J.G.; Supervision, Z.Y. and Z.Q.Y.

DECLARATION OF INTERESTS

The authors declare no conflict of interest.

Received: March 15, 2023
Revised: July 24, 2023
Accepted: September 6, 2023
Published: September 9, 2023

REFERENCES

1. Wienhold, S.-M., Macrì, M., Nouailles, G., Dietert, K., Gurtner, C., Gruber, A.D., Heimesaat, M.M., Lienau, J., Schumacher, F., Kleuser, B., et al. (2018). Ventilator-induced lung injury is aggravated by antibiotic mediated microbiota depletion in mice. Crit. Care *22*, 282. https://doi.org/10.1186/s13054-018-2213-8.
2. Wang, Y., Yang, Y., Chen, L., Xiong, W., Song, L., Li, B., Zhou, T., Pei, L., Yuan, S., Yao, S., and Shang, Y. (2020). Death-associated Protein Kinase 1 Mediates Ventilator-induced Lung Injury in Mice by Promoting Alveolar Epithelial Cell Apoptosis. Anesthesiology *133*, 905–918. https://doi.org/10.1097/ALN.0000000000003464.
3. Borges, J.B., Costa, E.L.V., Suarez-Sipmann, F., Widström, C., Larsson, A., Amato, M., and Hedenstierna, G. (2014). Early inflammation mainly affects normally and poorly aerated lung in experimental ventilator-induced lung injury. Crit. Care Med. *42*, e279–e287. https://doi.org/10.1097/CCM.0000000000000161.
4. Curley, G.F., Laffey, J.G., Zhang, H., and Slutsky, A.S. (2016). Biotrauma and Ventilator-Induced Lung Injury. Chest *150*, 1109–1117. https://doi.org/10.1016/j.chest.2016.07.019.
5. Lin, J.-Y., Jing, R., Lin, F., Ge, W.-Y., Dai, H.-J., and Pan, L. (2018). High Tidal Volume Induces Mitochondria Damage and Releases Mitochondrial DNA to Aggravate the Ventilator-Induced Lung Injury. Front. Immunol. *9*, 1477. https://doi.org/10.3389/fimmu.2018.01477.
6. Wang, L., Zhang, N., Zhang, Y., Xia, J., Zhan, Q., and Wang, C. (2018). Landscape of transcription and long non-coding RNAs reveals new insights into the inflammatory and fibrotic response following ventilator-induced lung injury. Respir. Res. *19*, 122. https://doi.org/10.1186/s12931-018-0822-z.
7. Kwack, W.G., Lee, Y.J., Eo, E.Y., Chung, J.H., Lee, J.H., and Cho, Y.J. (2021). Simultaneous Pretreatment of Aspirin and Omega-3 Fatty Acid Attenuates Nuclear Factor-kappaB Activation in a Murine Model with Ventilator-Induced Lung Injury. Nutrients *13*, 2258. https://doi.org/10.3390/nu13072258.
8. Chen, Z., He, S., Lian, S., Shen, Y., Jiang, W., Zhou, L., Zhou, L., and Zhang, X. (2023). The Wnt/beta-catenin pathway regulates inflammation and apoptosis in ventilator-induced lung injury. Biosci. Rep. *43*. https://doi.org/10.1042/BSR20222429.
9. Plötz, F.B., Slutsky, A.S., van Vught, A.J., and Heijnen, C.J. (2004). Ventilator-induced lung injury and multiple system organ failure: a critical review of facts and hypotheses. Intensive Care Med. *30*, 1865–1872. https://doi.org/10.1007/s00134-004-2363-9.
10. Muvhulawa, N., Dludla, P.V., Ziqubu, K., Mthembu, S.X.H., Mthiyane, F., Nkambule, B.B., and Mazibuko-Mbeje, S.E. (2022). Rutin ameliorates inflammation and improves metabolic function: A comprehensive analysis of scientific literature. Pharmacol. Res. *178*, 106163. https://doi.org/10.1016/j.phrs.2022.106163.
11. Khajevand-Khazaei, M.R., Mohseni-Moghaddam, P., Hosseini, M., Gholami, L., Baluchnejadmojarad, T., and Roghani, M. (2018). Rutin, a quercetin glycoside, alleviates acute endotoxemic kidney injury in C57BL/6 mice via suppression of inflammation and up-regulation of antioxidants and SIRT1. Eur. J. Pharmacol. *833*, 307–313. https://doi.org/10.1016/j.ejphar.2018.06.019.
12. Yeh, C.-H., Yang, J.-J., Yang, M.-L., Li, Y.-C., and Kuan, Y.-H. (2014). Rutin decreases lipopolysaccharide-induced acute lung injury via inhibition of oxidative stress and the MAPK–NF-κB pathway. Free Radic. Biol. Med. *69*, 249–257. https://doi.org/10.1016/j.freeradbiomed.2014.01.028.
13. Bispo da Silva, A., Cerqueira Coelho, P.L., Alves Oliveira Amparo, J., Alves de Almeida Carneiro, M.M., Pereira Borges, J.M., Dos Santos Souza, C., Dias Costa, M.d.F., Mecha, M., Guaza Rodriguez, C., Amaral da Silva, V.D., and Lima Costa, S. (2017). The flavonoid rutin modulates microglial/macrophage activation to a CD150/CD206 M2 phenotype. Chem. Biol. Interact. *274*, 89–99. https://doi.org/10.1016/j.cbi.2017.07.004.
14. Sharma, A., Tirpude, N.V., Kumari, M., and Padwad, Y. (2021). Rutin prevents inflammation-associated colon damage via inhibiting the p38/MAPKAPK2 and PI3K/Akt/GSK3beta/NF-kappaB signalling axes and enhancing splenic Tregs in DSS-induced murine chronic colitis. Food Funct. *12*, 8492–8506. https://doi.org/10.1039/d1fo01557e.
15. Qu, S., Dai, C., Lang, F., Hu, L., Tang, Q., Wang, H., Zhang, Y., and Hao, Z. (2019). Rutin Attenuates Vancomycin-Induced Nephrotoxicity by Ameliorating Oxidative Stress, Apoptosis, and Inflammation in Rats. Antimicrob. Agents Chemother. *63*, e01545-18. https://doi.org/10.1128/AAC.01545-18.
16. Oluranti, O.I., Alabi, B.A., Michael, O.S., Ojo, A.O., and Fatokun, B.P. (2021). Rutin prevents cardiac oxidative stress and inflammation induced by bisphenol A and dibutyl phthalate exposure via NRF-2/NF-kappaB pathway. Life Sci. *284*, 119878. https://doi.org/10.1016/j.lfs.2021.119878.
17. Huang, Y.C., Horng, C.T., Chen, S.T., Lee, S.S., Yang, M.L., Lee, C.Y., Kuo, W.H., Yeh, C.H., and Kuan, Y.H. (2016). Rutin improves endotoxin-induced acute lung injury via inhibition of iNOS and VCAM-1 expression. Environ. Toxicol. *31*, 185–191. https://doi.org/10.1002/tox.22033.
18. Yeh, C.H., Yang, J.J., Yang, M.L., Li, Y.C., and Kuan, Y.H. (2014). Rutin decreases lipopolysaccharide-induced acute lung injury via inhibition of oxidative stress and the MAPK-NF-kappaB pathway. Free Radic. Biol. Med. *69*, 249–257. https://doi.org/10.1016/j.freeradbiomed.2014.01.028.
19. Chen, W.Y., Huang, Y.C., Yang, M.L., Lee, C.Y., Chen, C.J., Yeh, C.H., Pan, P.H., Horng, C.T., Kuo, W.H., and Kuan, Y.H. (2014). Protective effect of rutin on LPS-induced acute lung injury via down-regulation of MIP-2 expression and MMP-9 activation through inhibition of Akt phosphorylation. Int. Immunopharmacol. *22*, 409–413. https://doi.org/10.1016/j.intimp.2014.07.026.
20. Su, K., Bo, L., Jiang, C., Deng, X., Zhao, Y.-Y., Minshall, R.D., and Hu, G. (2021). TLR4 is required for macrophage efferocytosis during resolution of ventilator-induced lung injury. Am. J. Physiol. Lung Cell Mol. Physiol. *321*, L787–L801. https://doi.org/10.1152/ajplung.00226.2021.
21. Liu, P., Yang, S., Wang, Z., Dai, H., and Wang, C. (2021). Feasibility and Mechanism Analysis of Shenfu Injection in the Treatment of Idiopathic Pulmonary Fibrosis. Front. Pharmacol. *12*, 670146. https://doi.org/10.3389/fphar.2021.670146.
22. Jiang, H., Mao, T., Liu, Y., Tan, X., Sun, Z., Cheng, Y., Han, X., Zhang, Y., Wang, J., Shi, L., et al. (2022). Protective Effects and Mechanisms of Yinchen Linggui Zhugan Decoction in HFD-Induced Nonalcoholic Fatty Liver Disease Rats Based on Network Pharmacology and Experimental Verification. Front. Pharmacol. *13*, 908128. https://doi.org/10.3389/fphar.2022.908128.
23. Moldoveanu, T., and Czabotar, P.E. (2020). BAX, BAK, and BOK: A Coming of Age for the BCL-2 Family Effector Proteins. Cold Spring Harbor Perspect. Biol. *12*, a036319. https://doi.org/10.1101/cshperspect.a036319.
24. Chen, S., Xia, J., Zhan, Q., and Zhang, Y. (2022). Microarray Analysis Reveals the Changes in Circular RNA Expression and Molecular Mechanisms in Mice With Ventilator-Induced Lung Injury. Front. Physiol. *13*, 838196. https://doi.org/10.3389/fphys.2022.838196.
25. Zhang, N.N., Zhang, Y., Wang, L., Xia, J.G., Liang, S.T., Wang, Y., Wang, Z.Z., Huang, X., Li, M., Zeng, H., and Zhan, Q.Y. (2019). Expression profiling analysis of long noncoding RNAs in a mouse model of ventilator-induced lung injury indicating potential roles in inflammation. J. Cell. Biochem. *120*, 11660–11679. https://doi.org/10.1002/jcb.28446.
26. Chen, S., Zhang, Y., and Zhan, Q. (2022). [Bioinformatics analysis of ventilator-induced lung injury genome microarray based on gene expression omnibus database and key gene verification]. Zhonghua Wei Zhong Bing Ji Jiu Yi Xue *34*, 41–47. https://doi.org/10.3760/cma.j.cn121430-20210823-01260.
27. Wang, L., Zhang, Y., Zhang, N., Xia, J., Zhan, Q., and Wang, C. (2019). Potential role of M2 macrophage polarization in ventilator-induced lung fibrosis. Int. Immunopharmacol. *75*, 105795. https://doi.org/10.1016/j.intimp.2019.105795.

28. Tian, C., Liu, X., Chang, Y., Wang, R., Yang, M., and Liu, M. (2021). Rutin prevents inflammation induced by lipopolysaccharide in RAW 264.7 cells via conquering the TLR4-MyD88-TRAF6-NF-kappaB signalling pathway. J. Pharm. Pharmacol. *73*, 110–117. https://doi.org/10.1093/jpp/rgaa015.
29. Nadella, V., Ranjan, R., Senthilkumaran, B., Qadri, S.S.Y.H., Pothani, S., Singh, A.K., Gupta, M.L., and Prakash, H. (2019). Podophyllotoxin and Rutin Modulate M1 (iNOS+) Macrophages and Mitigate Lethal Radiation (LR) Induced Inflammatory Responses in Mice. Front. Immunol. *10*, 106. https://doi.org/10.3389/fimmu.2019.00106.
30. Su, K.Y., Yu, C.Y., Chen, Y.P., Hua, K.F., and Chen, Y.L.S. (2014). 3,4-Dihydroxytoluene, a metabolite of rutin, inhibits inflammatory responses in lipopolysaccharide-activated macrophages by reducing the activation of NF-kappaB signaling. BMC Compl. Alternative Med. *14*, 21. https://doi.org/10.1186/1472-6882-14-21.
31. Wang, L., Zhang, H., Sun, L., Gao, W., Xiong, Y., Ma, A., Liu, X., Shen, L., Li, Q., and Yang, H. (2020). Manipulation of macrophage polarization by peptide-coated gold nanoparticles and its protective effects on acute lung injury. J. Nanobiotechnol. *18*, 38. https://doi.org/10.1186/s12951-020-00593-7.
32. Schappe, M.S., Szteyn, K., Stremska, M.E., Mendu, S.K., Downs, T.K., Seegren, P.V., Mahoney, M.A., Dixit, S., Krupa, J.K., Stipes, E.J., et al. (2018). Chanzyme TRPM7 Mediates the Ca(2+) Influx Essential for Lipopolysaccharide-Induced Toll-Like Receptor 4 Endocytosis and Macrophage Activation. Immunity *48*, 59–74.e5. https://doi.org/10.1016/j.immuni.2017.11.026.
33. Oishi, Y., Spann, N.J., Link, V.M., Muse, E.D., Strid, T., Edillor, C., Kolar, M.J., Matsuzaka, T., Hayakawa, S., Tao, J., et al. (2017). SREBP1 Contributes to Resolution of Pro-inflammatory TLR4 Signaling by Reprogramming Fatty Acid Metabolism. Cell Metabol. *25*, 412–427. https://doi.org/10.1016/j.cmet.2016.11.009.
34. Wu, J., Yan, Z., Schwartz, D.E., Yu, J., Malik, A.B., and Hu, G. (2013). Activation of NLRP3 Inflammasome in Alveolar Macrophages Contributes to Mechanical Stretch-Induced Lung Inflammation and Injury. J. Immunol. *190*, 3590–3599. https://doi.org/10.4049/jimmunol.1200860.
35. Hosseinian, N., Cho, Y., Lockey, R.F., and Kolliputi, N. (2015). The role of the NLRP3 inflammasome in pulmonary diseases. Ther. Adv. Respir. Dis. *9*, 188–197. https://doi.org/10.1177/1753465815586335.
36. Zhang, Y., Liu, G., Dull, R.O., Schwartz, D.E., and Hu, G. (2014). Autophagy in pulmonary macrophages mediates lung inflammatory injury via NLRP3 inflammasome activation during mechanical ventilation. Am. J. Physiol. Lung Cell Mol. Physiol. *307*, L173–L185. https://doi.org/10.1152/ajplung.00083.2014.
37. An, X., Sun, X., Yang, X., Liu, D., Hou, Y., Chen, H., and Wu, J. (2019). Oxidative stress promotes ventilator-induced lung injury through activating NLRP3 inflammasome and TRPM2 channel. Artif. Cells, Nanomed. Biotechnol. *47*, 3448–3455. https://doi.org/10.1080/21691401.2019.1652631.
38. Liu, H., Gu, C., Liu, M., Liu, G., Wang, D., Liu, X., and Wang, Y. (2019). Ventilator-induced lung injury is alleviated by inhibiting NLRP3 inflammasome activation. Mol. Immunol. *111*, 1–10. https://doi.org/10.1016/j.molimm.2019.03.011.
39. Tang, R., Hu, Y., Mei, S., Zhou, Y., Feng, J., Jin, T., Dai, B., Xing, S., Gao, Y., Xu, Q., and He, Z. (2023). Non-coding RNA alterations in extracellular vesicles from bronchoalveolar lavage fluid contribute to mechanical ventilation-induced pulmonary fibrosis. Front. Immunol. *14*, 1141761. https://doi.org/10.3389/fimmu.2023.1141761.
40. Liu, H., Gu, C., Liu, M., Liu, G., and Wang, Y. (2020). NEK7 mediated assembly and activation of NLRP3 inflammasome downstream of potassium efflux in ventilator-induced lung injury. Biochem. Pharmacol. *177*, 113998. https://doi.org/10.1016/j.bcp.2020.113998.
41. Verma, S., Kalita, B., Bajaj, S., Prakash, H., Singh, A.K., and Gupta, M.L. (2017). A Combination of Podophyllotoxin and Rutin Alleviates Radiation-Induced Pneumonitis and Fibrosis through Modulation of Lung Inflammation in Mice. Front. Immunol. *8*, 658. https://doi.org/10.3389/fimmu.2017.00658.
42. Colunga Biancatelli, R.M.L., Solopov, P.A., and Catravas, J.D. (2022). The Inflammasome NLR Family Pyrin Domain-Containing Protein 3 (NLRP3) as a Novel Therapeutic Target for Idiopathic Pulmonary Fibrosis. Am. J. Pathol. *192*, 837–846. https://doi.org/10.1016/j.ajpath.2022.03.003.
43. Guo, X., Ji, J., Feng, Z., Hou, X., Luo, Y., and Mei, Z. (2020). A network pharmacology approach to explore the potential targets underlying the effect of sinomenine on rheumatoid arthritis. Int. Immunopharmacol. *80*, 106201. https://doi.org/10.1016/j.intimp.2020.106201.
44. Liu, F., Li, Y., Yang, Y., Li, M., Du, Y., Zhang, Y., Wang, J., and Shi, Y. (2021). Study on mechanism of matrine in treatment of COVID-19 combined with liver injury by network pharmacology and molecular docking technology. Drug Deliv. *28*, 325–342. https://doi.org/10.1080/10717544.2021.1879313.
45. Zhou, Y., Zhou, B., Pache, L., Chang, M., Khodabakhshi, A.H., Tanaseichuk, O., Benner, C., and Chanda, S.K. (2019). Metascape provides a biologist-oriented resource for the analysis of systems-level datasets. Nat. Commun. *10*, 1523. https://doi.org/10.1038/s41467-019-09234-6.
46. Mi, H., Huang, X., Muruganujan, A., Tang, H., Mills, C., Kang, D., and Thomas, P.D. (2017). PANTHER version 11: expanded annotation data from Gene Ontology and Reactome pathways, and data analysis tool enhancements. Nucleic Acids Res. *45*, D183–D189. https://doi.org/10.1093/nar/gkw1138.
47. Zhang, J.D., and Wiemann, S. (2009). KEGGgraph: a graph approach to KEGG PATHWAY in R and bioconductor. Bioinformatics *25*, 1470–1471. https://doi.org/10.1093/bioinformatics/btp167.
48. Matute-Bello, G., Downey, G., Moore, B.B., Groshong, S.D., Matthay, M.A., Slutsky, A.S., and Kuebler, W.M.; Acute Lung Injury in Animals Study Group (2011). An official American Thoracic Society workshop report: features and measurements of experimental acute lung injury in animals. Am. J. Respir. Cell Mol. Biol. *44*, 725–738. https://doi.org/10.1165/rcmb.2009-0210ST.
49. Shah, D., Romero, F., Zhu, Y., Duong, M., Sun, J., Walsh, K., and Summer, R. (2015). C1q Deficiency Promotes Pulmonary Vascular Inflammation and Enhances the Susceptibility of the Lung Endothelium to Injury. J. Biol. Chem. *290*, 29642–29651. https://doi.org/10.1074/jbc.M115.690784.

STAR★METHODS

KEY RESOURCES TABLE

REAGENT or RESOURCE	SOURCE	IDENTIFIER
Antibodies		
Rabbit monoclonal to iNOS	Abcam	ab178945
Rabbit polyclonal to Mannose Receptor (CD206)	Abcam	ab64693
Rabbit monoclonal to Bax	Abcam	ab32503
Rabbit monoclonal to Bax	Abcam	ab182733
Rabbit monoclonal to Bcl-2	Abcam	ab182858
Rabbit polyclonal to NLRP3	Abcam	ab214185
Rabbit monoclonal to ASC	Cell Signaling Technology	67824
Rabbit polyclonal to Caspase-1	Abcam	ab138483
Rabbit polyclonal to TLR4	Abcam	ab13867
Rabbit polyclonal to MD2	Abcam	ab24182
Rabbit polyclonal to NF-kB p65	Abcam	ab16502
Rabbit monoclonal to Phospho-NFkB p65 (Ser536)	Thermo Fisher Scientific	MA5-15160
Rabbit monoclonal to NLRP3	Abcam	ab270449
Rabbit monoclonal to pro Caspase-1 + p10 + p12	Abcam	ab179515
CD45 Monoclonal Antibody (30-F11), FITC, eBioscience™	Thermo Fisher Scientific	11-0451-81
Chemicals, peptides, and recombinant proteins		
Rutin	MedChemExpress, MCE	HY-N0148
Critical commercial assays		
TUNEL Apoptosis Assay Kit	Roche	11684817910
DAPI	Abcam	ab104139
RIPA lysis buffer	Cell Signaling Technology	Cat#9806
protease inhibitor	Sigma	539131
bicinchoninic acid (BCA) protein assay kit	Thermo Fisher Scientific	23227
chemiluminescent substrate	Thermo Fisher Scientific	34577
TRIzol reagent	Invitrogen Life Technologies	15596026
TaqMan reverse transcription kit	TaKaRa	RR036A
SYBR® PremixEx Taq II Kit	TaKaRa	RR420A
Deposited data		
Raw and analyzed data	This paper	iScience-D-23-01386
Experimental models: Organisms/strains		
Mouse:C57BL/6J	Purchased from Beijing Sipeifu Biotechnology Co., Ltd., China	No.11032421106635446
Oligonucleotides		
Primers for TLR4, MD2, P65, NLRP3, ASC, Caspase-1, IL1β, IL18, GAPDH	This paper	N/A
Software and algorithms		
ImageJ	Bethesda, MD, USA	https://imagej.nih.gov/ij/
Image-Pro Plus 6.0 System	Media Cybernetics, USA	https://www.mediacy.com/
AutoDockTools	The Scripps Research Institute, USA	https://autodock.scripps.edu/
PyMOL	Schrödinger, USA	https://pymol.org/2/

(*Continued on next page*)

Continued

REAGENT or RESOURCE	SOURCE	IDENTIFIER
Other		
Confocal laser scanning microscopy	Leica	https://www.leica-microsystems.com.cn/
PubChem	This paper	https://pubchem.ncbi.nlm.nih.gov/
TCMSP database	This paper	http://tcmspw.com
Swiss Target Prediction database	This paper	http://www.swisstargetprediction.ch/
TargetNet web server database	This paper	http://targetnet.scbdd.com/home/index/
SymMap database	This paper	https://www.symmap.org/
UniProt database	This paper	https://www.uniprot.org
GeneCards database	This paper	https://www.genecards.org
DisGeNET	This paper	http://www.disgenet.org
Venn analysis tool	This paper	http://bioinformatics.psb.ugent.be/webtools/Venn/
Metascape platform analysis tool	This paper	http://metascape.org/gp/index.html#/main/step1
DAVID database	This paper	https://david.ncifcrf.gov/
RCSB PDB database	This paper	https://www.rcsb.org/

RESOURCE AVAILABILITY

Lead contact

Further information or requests for resources and reagents should be directed to the lead author, Qingyuan Zhan (drzhanqy@163.com).

Materials availability

This study did not generate any unique reagents or materials.

Data and code availability

- All data reported in this paper will be shared by the corresponding authors upon request.
- This paper does not report original code.
- Any additional information required to reanalyze the data reported in this paper is available from the lead contact upon request.

EXPERIMENTAL MODEL AND SUBJECT DETAILS

Animals

Male C57BL/6 mice (aged 8–10 weeks, weight 22 $\pm$ 2 g) were purchased from Beijing Sipeifu Biotechnology Co., Ltd., China. All mice were conventionally housed at 22 $\pm$ 2°C under a 12 h light–dark cycle with free access to water and food. All animal experiments were performed in compliance with the policies of the National Institutes of Health (NIH) Guide for the Care and Use of Laboratory Animals and were approved by the Experimental Animal Ethics Committee of China-Japan Friendship Hospital.

Mouse model of VILI and rutin treatment

The mouse VILI model was established according to our previous studies.[24,25] Briefly, the experimental mice were anesthetized with 1% sodium pentobarbital (100 mg/kg), and a tracheotomy was performed. A 22G trocar (BD Biosciences, United States) was inserted, and the trachea was ligated to prevent air leakage. Continuous mechanical ventilation was performed for 4 h using a small animal ventilator (Harvard Apparatus, United States). Sodium pentobarbital and rocuronium benzenesulfonic acid (0.6 mg/kg) were used to maintain anesthesia and muscle relaxation, respectively. Mice in the control group were intubated but not ventilated. The mice were sacrificed 6 h after ventilation, and the lungs were perfused and isolated for subsequent analyses. Bronchoalveolar lavage fluid (BALF) were collected for further analysis.

Forty mice were randomly divided into four groups of 10 mice each, including the control group, VILI group, VILI + rutin group and rutin group. The experimental procedures are described in below figure. Mice in the control group were given 500 μL of PBS by intraperitoneal (i.p.) injection for three days and then were intubated without ventilation for 4 h. Mice in the VILI group were given 500 μL of PBS by i.p. injection for three days and then underwent mechanical ventilation for 4 h. Mice in the VILI + rutin group were given 500 μL of rutin (0.5 mM) by i.p. injection for three days and then underwent mechanical ventilation for 4 h. Mice in the rutin group were given 500 μL of rutin (0.5 mM) by i.p. injection for

three days and then underwent intubation without ventilation for 4 h. Rutin (MCE, USA) was dissolved in DMSO, and the mice were administered an intraperitoneal (i.p.) injection in a volume of 500 μL for three consecutive days.[17,18]

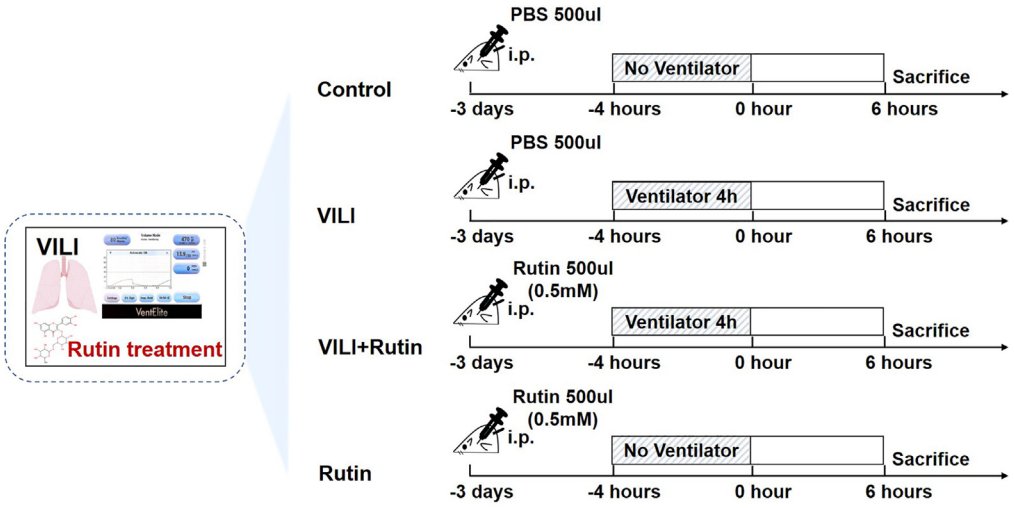

METHOD DETAILS

Rutin chemical structures

PubChem (https: pubchem.ncbi.nlm.nih.gov) is an open chemical database that provides information about compound structures and descriptive data.[43] The PubChem database was used to search the 2D chemical structure of rutin.

Prediction of the targets of rutin

Four databases were used to screen the potential targets of rutin.[43,44] They were the TCMSP database (http://tcmspw.com), Swiss Target Prediction database (http://www.swisstargetprediction.ch/, SWISS), TargetNet web server database (http://targetnet.scbdd.com/home/index/, TargetNet) and SymMap database (https://www.symmap.org/, SymMap). The gene names corresponding to the candidate targets were then obtained from the UniProt database (https://www.uniprot.org).

Prediction of targets for VILI

Two databases were used to identify the potential targets of VILI.[43,44] They were the GeneCards database (https://www.genecards.org) and genetic disease association database (DisGeNET, http://www.disgenet.org). Ventilator-induced lung injury was set as the keyword and deduplicated, and potential targets for the prevention and treatment of VILI were acquired from the two databases.

Prediction of therapeutic targets of rutin in the treatment of VILI

The online Venn analysis tool (http://bioinformatics.psb.ugent.be/webtools/Venn/) was used to calculate and draw custom Venn diagrams to obtain the common targets of rutin in the treatment of VILI.

Construction of the protein–protein interaction (PPI) network

The Metascape platform analysis tool (metascape.org/gp/index.html#/main/step1) was used for PPI analysis.[45] The common target genes of rutin and VILI were uploaded to Metascape, and PPIs were obtained based on a minimum overlap value of three and a p value cutoff less than 0.01.

Gene Ontology and KEGG pathway analysis

Gene Ontology (GO) is an internationally standardized classification system of gene functions and is used to evaluate gene functions and interrelationships among the functions of different genes.[46] KEGG pathway analysis is a high-level functional and utility analysis of biological systems and is used to study biological effects and multidimensional pharmacological mechanisms at the pathway level.[47] GO analysis and KEGG analyses were performed to enrich the functions of the potential targets of rutin in the treatment of VILI in terms of biological process (BP), molecular function (MF), cellular components (CC) and enriched pathways using the DAVID database (https://david.ncifcrf.gov/) The organism selected was *Homo sapiens*. GO terms with corrected values of $p < 0.05$ were considered significantly enriched in differentially expressed genes. KEGG pathways with a $p < 0.05$ were defined as being significantly enriched. The results are shown in bubble charts.

Molecular docking

AutoDockTools was used for the docking analysis of the representative compounds and targets. The cocrystallized X-ray structures of the target proteins were obtained from the RCSB PDB database (https://www.rcsb.org/) and were used as the binding cavities of proteins. The active components of rutin were obtained from the PubChem database (https://pubchem.ncbi.nlm.nih.gov/) and were used as ligands. Water molecule removal, nonpolar hydrogen addition and the calculation of the affinities between these proteins and ligands were completed by AutoDockTools (v 1.5.7) software. Both target and receptor molecules were saved in pdbqt format after combining nonpolar hydrogens. The docking results were visualized using PyMOL (v 2 5.2) software.

Hematoxylin-eosin (HE) staining

Lung tissues were collected and fixed in 4% paraformaldehyde. Then, 5-μm sections were cut from paraffin tissue blocks, stained with HE and observed under an optical microscope (Olympus, Japan). The lung injury score was calculated by two researchers who were blinded to the group information as described previously.[48] Five independent variables, including neutrophils in the alveolar space, neutrophils in the interstitial space, the existence of hyaline membranes, proteinaceous debris filling the airspaces and alveolar septal thickening, were used to determine a lung injury score.

Measurement of protein concentrations and cell count in BALF

Bronchoalveolar lavage was performed 6 h after ventilation by cannulating the trachea with a blunt 22-gauge needle and instilling 1 mL PBS into the lung three times.[49] Total cell count was determined by flow cytometry detection with CD45 (Thermo, 11-0451-81, USA), a marker of white blood cell (WBC). Briefly, BALF was centrifuged at room temperature for 5 min and BALF supernatant and cell precipitation were collected separately. Cell precipitation was incubated with CD45 antibody for 20 min at room temperature and then washed twice in PBS. Cells were resuspended in 500 μL PBS and was analyzed with flow cytometry (Beckman, USA). Total protein concentration in the BALF supernatant was determined using a bicinchoninic acid (BCA) protein assay kit (Thermo Scientific, USA).

TUNEL staining

Lung tissues were collected and fixed in 4% paraformaldehyde. Then, 5-μm sections were cut from paraffin tissue blocks, stained with TUNEL according to the manufacturer's instructions and observed under a fluorescence microscope (Olympus, Japan); 10 fields of view were randomly selected, and the rate of cell apoptosis was determined using ImageJ (Bethesda, MD, USA). Green nuclei were considered apoptotic cells. Cells with blue nuclei were deemed normal, and the average value was determined accordingly. The ratio of the number of green cells to that of blue cells was regarded as the rate of cell apoptosis.

Immunofluorescence and immunohistochemical staining

Lung tissues were collected and fixed in 4% paraformaldehyde, and immunofluorescence (IF) staining was performed to evaluate iNOS and CD206 expression in lung tissues according to the manufacturer's protocol. Briefly, tissue specimens were cut into 5-μm serial sections and blocked with 10% blocking serum in PBS. The sections were then incubated with primary antibodies against iNOS (Abcam, ab178945, UK) and CD206 (Abcam, ab64693, UK) at 4°C overnight. The sections were incubated with Alexa Fluor 488-conjugated goat anti-rabbit IgG secondary antibodies and Alexa Fluor Plus 555-conjugated goat anti-rabbit IgG secondary antibodies (Molecular Probes, Invitrogen, USA) for 1 h at room temperature. DAPI (Abcam, UK) was used for nuclear staining. The sections were observed with a fluorescence microscope (Olympus, Japan), and the images were analyzed using ImageJ (Bethesda, MD, USA).

Lung tissues were collected and fixed in 4% paraformaldehyde, and immunohistochemical (IHC) staining was used to evaluate B-cell lymphoma 2 (Bcl2), Bcl2-associated protein x (Bax), NLRP3, ASC, Caspase1, TLR4, MD2, p-P65 and P65 expression in lung tissues according to the manufacturer's protocol. Briefly, tissue specimens were cut into 5-μm serial sections, deparaffinized, rehydrated, blocked and incubated with primary antibodies against Bax (Abcam, ab32503, UK), Bcl2 (Abcam, ab182858, UK), NLRP3 (Abcam, ab214185, UK), ASC (CST, 67824, USA), Caspase1 (Abcam, ab138483, UK), TLR4 (Abcam, ab13867, UK), MD2 (Abcam, ab24182, UK), p-P65 (Thermo, MA5-15160, USA) and P65 (Abcam, ab16502, UK) at 4°C overnight. The sections were incubated with biotinylated IgG (1:250) for 1 h and then with streptavidin-HRP for 30 min at room temperature. DAB was then added to each section and incubated for 5 min. The sections were observed with a microscope (Olympus, Japan), and the images were analyzed using Image-Pro Plus 6.0 (Media Cybernetics, USA).

Western blot analysis

Total protein was extracted using RIPA lysis buffer (Cell Signaling Technology, USA) containing a protease inhibitor (Sigma, USA), and protein concentrations were measured using a bicinchoninic acid (BCA) protein assay kit (Thermo Scientific, USA). Equal amounts of total protein (50 μg) were separated by SDS–PAGE and electrotransferred to a PVDF membrane. The membranes were incubated with the following primary antibodies: Bax (Abcam, ab182733, UK), Bcl2 (Abcam, ab182858, UK), NLRP3 (Abcam, ab270449, UK), ASC (CST, 67824, USA), Caspase1 (Abcam, ab179515, UK), TLR4 (Abcam, ab13867, UK), MD2 (Abcam, ab24182, UK), p-P65 (Thermo, MA5-15160, USA) and P65 (Abcam, ab16502, UK). The antibody complexes were visualized with a chemiluminescent substrate (Thermo Scientific, USA) using a ChemiDoc XRS device (Bio-Rad, USA). For quantification, electrochemiluminescence (ECL) signals were digitized using Quantity One software.

Real-time PCR

Total RNA was extracted from lung tissue using TRIzol reagent (Invitrogen Life Technologies, Carlsbad, CA) according to the manufacturer's protocol. cDNA synthesis was performed using random hexamer primers and a TaqMan reverse transcription kit (TaKaRa, Japan). Quantitative real-time PCR was performed using an SYBR PremixEx Taq II Kit (TaKaRa, Japan) on a 7500 Fast Real-Time PCR system from Applied Biosystems (Bio-Rad, USA). The relative gene expression levels were determined by the ΔΔCt method using GAPDH as a reference gene. All primer sequences are listed in below table.

Primer sequence used for RT-PCR analysis

Genes	Primer sequence (5′→3′)
TLR4	Fwd 5′-GCCATCATTATGAGTGCCAATT-3′ Rev 5′-AGGGATAAGAACGCTGAGAATT-3′
MD2	Fwd 5′-CTGAATCTGAGAAGCAACAGTG-3′ Rev 5′-CTTGGAATGAACTCAACATGCA-3′
P65	Fwd 5′-AGACCCAGGAGTGTTCACAGACC-3′ Rev 5′-GTCACCAGGCGAGTTATAGCTTCAG-3′
NLRP3	Fwd 5′-GCCGTCTACGTCTTCTTCCTTTCC-3′ Rev 5′-CATCCGCAGCCAGTGAACAGAG-3′
ASC	Fwd 5′-ACAATGACTGTGCTTAGAGACA-3′ Rev 5′-CACAGCTCCAGACTCTTCTTTA-3′
Caspase1	Fwd 5′-AGAGGATTTCTTAACGGATGCA-3′ Rev 5′-TCACAAGACCAGGCATATTCTT-3′
IL1β	Fwd 5′-CACTACAGGCTCCGAGATGAACAAC-3′ Rev 5′-TGTCGTTGCTTGGTTCTCCTTGTAC-3′
IL18	Fwd 5′-AGACCTGGAATCAGACAACTTT-3′ Rev 5′-TCAGTCATATCCTCGAACACAG-3′
GAPDH	Fwd 5′-GGTTGTCTCCTGCGACTTCA-3′ Rev 5′-TGGTCCAGGGTTTCTTACTCC-3′

QUANTIFICATION AND STATISTICAL ANALYSIS

The data are presented as the means ± SEMs. n = biological replicates. One-way ANOVA was used to analyze statistical significance as appropriate. $p < 0.05$ was considered statistically significant. The statistical analyses were performed using Statistical Product and Service Solutions (SPSS) 19.0 (Systat Software, San Jose, CA, USA).